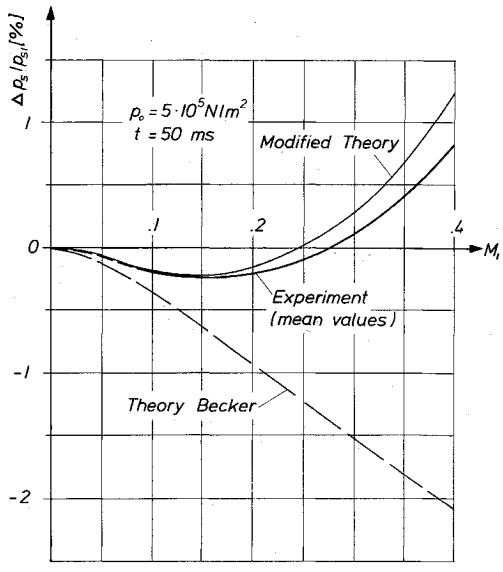

Fig. 4 Stagnation pressure variation vs Mach number.

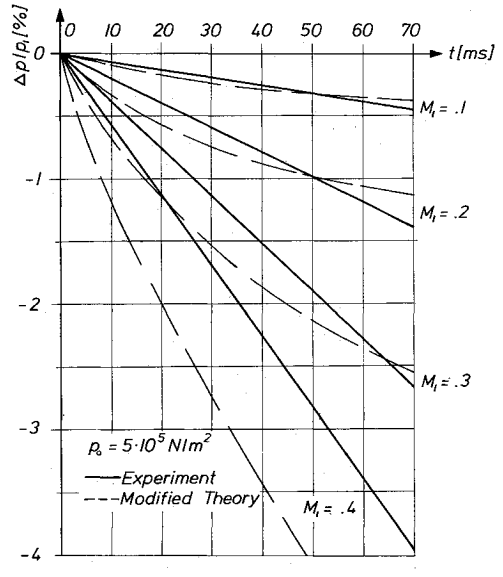

Fig. 5 Static pressure vs time.

measured. Therefore the original theory should be modified by accepting some different assumptions. One of the most important modifications was the inclusion of the curvature-effect of the tube wall on the mass sources which result from the boundary-layer growth. So the theoretical treatment can be extended to longer running times (thicker boundary layers). The results are typically shown in Fig. 3 and 4 for the variations of static and stagnation pressure ahead of the nozzle as functions of Mach number at a running time of 50 msec after opening of the diaphragm (see Fig. 2). The different curves shown follow mean values of the experimental data, Becker's original theory, and the modified theory which is presented in detail in Ref. 2. For low Mach numbers the agreement between the modified theory and the experiments is good. It should not be concealed, however, that the parameter t chosen in Fig. 3 and 4 leads to rather favorable results. For other running times the agreement is poorer. This can be seen from Fig. 5 for the static pressure variation at different Mach numbers. For short running times the pressure drop is overestimated. The reason is that the flow is assumed to be set into motion by an "expansion shock" of zero extent rather than a finite width expansion wave. Later this effect is lessened to give a favorable prediction of the pressure variation.

Summary

To estimate the variations of static and stagnation pressure at the nozzle inlet of a Ludwieg Tube due to boundary-layer growth Becker's modified theory is recommended as it is described in Ref. 2. Moreover the variations of other thermodynamic properties of the operating gas can be computed without difficulty. By systematic linearization in terms of the Mach number M_1 the numerical treatment of Becker's theory is considerably simplified and can be handled on a desk computer.

For calculation which is valid for a specific heat ratio $\gamma = 1.4$ the following steps have to be taken. 1) Boundary-layer growth at the nozzle (Kàrmàn-Pohlhausen-Method)

$$\delta_N(t) = 0.303M_1{}^{3/5}(1 - 0.623M_1)\{(v_{oo}/a_o)(p_{at}/p_o)\}^{1/5}(a_o t)^{4/5}$$

2) From the solution of the inhomogeneous wave equation

$$\Delta p'/p_1 = 0.123M_1(1 - 0.064M_1)(1 + \tfrac{1}{2}\delta_N/r + \tfrac{1}{3}\delta_N^2/r^2)\,\delta_N/r$$

(primary compression waves being directly caused by the boundary-layer). 3) Boundary condition $M = 1$ in the nozzle throat

$$\frac{M(t)}{[1 + 0.2M(t)^2]^3} = \frac{M_1}{(1 + 0.2M_1{}^2)^3}\left(\frac{1 - \varphi(M_1)\,\delta_N^*/r}{1 - \delta_N^*/r}\right)^2$$

where

$$\varphi(M_1) = 1.31M_1{}^{5/2}(1 - 0.24M_1); \quad \delta_N^* = 0.125(1 + 0.311M_1)\delta_N$$

4) Because of reflected waves at the nozzle

$$\frac{\Delta p''}{p_1} = \frac{7}{5}\frac{M_1 + \frac{5}{7}\Delta p'/p_1 - M(t)(1 - \frac{1}{7}\Delta p'/p_1)}{1 + 0.2M(t)}$$

5) Resultant pressure and stagnation pressure variations are

$$\Delta p/p_1 = (\Delta p' + \Delta p'')/p_1$$

and

$$\Delta p_s/p_{s1} = \left[\frac{1 + 0.2M(t)^2}{1 + 0.2M_1{}^2}\right]^{3.5}(1 + \Delta p/p_1) - 1$$

References

[1] Becker, E., "Reibungswirkungen im Rohrwindkanal," Mitteilungen aus dem Max-Planck-Institut fur Stroemungsforschung und der Aerodynamischen Versuchsanstalt, Nr. 20, Goettingen, 1958.

[2] Piltz, E., "Druckaenderungen als Grenzschichteffekte im Rohrwindkanal," Dissertation Technische Hochschule Darmstadt, 1971.

Proper Equations and Similar Approximations in the Hypersonic Merged Layer

MOHAMED NABIH WAGDI*
University of Cairo, Cairo, Egypt

Nomenclature

f = nondimensional stream function
H = total enthalpy
M_∞ = freestream Mach number
p = static pressure
Pr = Prandtl number
Re/x = Reynolds number per unit length x
U_∞ = freestream velocity
T = static temperature
u = streamwise velocity component
v = normal velocity component
x = streamwise coordinate

Received December 7, 1971; revision received March 18, 1972.
Index categories: Supersonic and Hypersonic Flow; Viscous Non-boundary-Layer Flows.

* Associate Professor, Department of Aeronautical Engineering; presently on leave to The College of Engineering, University of Riyadh, Kingdom of Saudi Arabia. Member AIAA.

y = normal coordinate
ε = hypersonic density ratio $(\gamma-1)/(\gamma+1)$
γ = specific heat ratio
μ = coefficient of viscosity
ρ = density
η = nondimensional normal coordinate

Superscripts

$-$ = nondimensional quantities refer to freestream conditions
(0) = zero-order approximation
(1) = first-order approximation

Subscripts

0 = zero-order flow parameters
1 = first-order flow parameters
w = wall conditions
∞ = freestream conditions

Introduction

IN studying the flow characteristics in the merged layer region of a pointed body moving at hypersonic speed, the conventional boundary-layer theory cannot be used. In the merged layer region, the boundary-layer principle assumptions are violated. Moreover, boundary-layer secondary effects do not even adequately describe the flow characteristics in the region. Thus we must resort to the more general Navier-Stokes equations. Dealing with such equations is a matter of great, if not, of formidable difficulty.

To produce a system which lends itself to mathematical analysis (whether numerical or analytical), we have to simplify the Navier-Stokes equations, witout jeopardizing the physical behavior of the problem. This can be achieved by performing an order of magnitude analysis, where the terms of minor effect may be dropped, while retaining other important terms. To do so, use is made of known experimental and analytical results to define some reference parameters.

In the merged layer region, the shock wave is almost straight.[1] In spite of the fact that the shock-wave layer is not thin compared to the inner viscous layer, we can assume without introducing appreciable error, that the shock slope $y_s/x = 0(\varepsilon^{1/2})$. The pressure, temperature, and density behind the shock layer are $p_s = 0(p_\infty \varepsilon M_\infty{}^2)$, $T_s = 0(T_\infty \varepsilon M_\infty{}^2)$, and $\rho_s = 0(\rho_\infty)$, respectively.

The velocity at the inner face of the shock layer is the sum of the tangential velocity component and the shear stress,[2] due to slip effects. The upper boundary of the merged layer could be adequately described by $M_\infty/Re_x{}^{1/2} = 0(1)$, while the lower bound is characterized[3,4] by $M_\infty{}^2/Re_x = 0(1)$.

Analysis

Considering a two dimensional configuration, the Navier-Stokes equations in Cartesian coordinate system are

$$\frac{Du}{Dt} = -\frac{1}{\rho}\frac{\partial p}{\partial x} - \frac{1}{\rho}\left\{\frac{2}{3}\frac{\partial}{\partial x}\left(\mu\frac{\partial v}{\partial y}\right) - \frac{4}{3}\frac{\partial}{\partial x}\left(\mu\frac{\partial u}{\partial x}\right) - \frac{\partial}{\partial y}\left[\mu\left(\frac{\partial u}{\partial y}+\frac{\partial v}{\partial x}\right)\right]\right\} \tag{1a}$$

$$\frac{Dv}{Dt} = -\frac{1}{\rho}\frac{\partial p}{\partial y} - \frac{1}{\rho}\left\{\frac{2}{3}\frac{\partial}{\partial y}\left(\mu\frac{\partial u}{\partial x}\right) - \frac{4}{3}\frac{\partial}{\partial y}\left(\mu\frac{\partial v}{\partial y}\right) - \frac{\partial}{\partial x}\left[\mu\left(\frac{\partial v}{\partial x}+\frac{\partial u}{\partial y}\right)\right]\right\} \tag{1b}$$

and the energy equation is

$$\rho u\frac{\partial H}{\partial x} + \rho v\frac{\partial H}{\partial y} = \frac{\partial}{\partial y}\left(\mu\frac{\partial H}{\partial y}\right) + \frac{\partial}{\partial y}\left[\left(\frac{1}{Pr}-1\right)\mu\frac{\partial}{\partial y}(H-u^2/2)\right] \tag{1c}$$

Introducing series expansions of the flow parameters in terms of ε

$$\begin{gathered}\bar{u} = u/U_\infty = u_0\varepsilon^{-1} + u_1 + u_2\varepsilon + \ldots \\ \bar{v} = v/U_\infty = v_0\varepsilon^{-1/2} + v_1\varepsilon^{1/2} + v_2\varepsilon^{3/2} + \ldots \\ \bar{p} = p/p_\infty = \varepsilon p_0; \quad \bar{T} = T/T_\infty = \varepsilon T_0; \quad \bar{\rho} = \rho/\rho_\infty \\ \bar{\mu} = \mu/\mu_\infty = \varepsilon\mu_0 \\ \bar{H} = 2H/U_\infty{}^2 = H_0\varepsilon^{-2} + H_1\varepsilon^{-1} + H_2 + \ldots\end{gathered} \tag{2}$$

where subscripts denote order of the relevant parameters. Substituting Eqs. (2) into Eqs. (1) and collecting coefficients of equal powers of ε, we get, after the introduction of the transformation

$$\bar{x} = \left(\frac{Re/x}{M_\infty{}^2}\right)x \quad \text{and} \quad \bar{y} = \left(\frac{Re/x}{M_\infty{}^2}\right)(y/\varepsilon^{1/2}) \tag{3}$$

The zero-order approximation (coefficients of ε°) equations are

$$\frac{\partial}{\partial\bar{x}}(\bar{\rho}u_0) + \frac{\partial}{\partial\bar{y}}(\bar{\rho}v_0) = 0 \tag{4a}$$

$\bar{x}$ momentum:

$$u_0\frac{\partial u_0}{\partial\bar{x}} + v_0\frac{\partial u_0}{\partial\bar{y}} = \frac{1}{\bar{\rho}M_\infty{}^2}\frac{\partial}{\partial\bar{y}}\left(\mu_0\frac{\partial u_0}{\partial\bar{y}}\right) \tag{4b}$$

$\bar{y}$ momentum:

$$u_0\frac{\partial v_0}{\partial\bar{x}} + v_0\frac{\partial v_0}{\partial\bar{y}} = \frac{-1}{\bar{\rho}M_\infty{}^2}\left[\frac{1}{\gamma}\frac{\partial p_0}{\partial\bar{y}} + \frac{2}{3}\frac{\partial}{\partial\bar{y}}\left(\mu_0\frac{\partial u_0}{\partial\bar{x}}\right) - \frac{\partial}{\partial\bar{x}}\left(\mu_0\frac{\partial u_0}{\partial\bar{y}}\right) - \frac{4}{3}\frac{\partial}{\partial\bar{y}}\left(\mu_0\frac{\partial v_0}{\partial\bar{y}}\right)\right] \tag{4c}$$

energy:

$$u_0\frac{\partial H_0}{\partial\bar{x}} + v_0\frac{\partial H_0}{\partial\bar{y}} = \frac{1}{\bar{\rho}M_\infty{}^2}\left\{\frac{\partial}{\partial\bar{y}}\left(\mu_0\frac{\partial H_0}{\partial\bar{y}}\right) + \frac{\partial}{\partial\bar{y}}\times\left[\left(\frac{1}{Pr}-1\right)\mu_0\frac{\partial}{\partial\bar{y}}(H_0-u_0{}^2)\right]\right\} \tag{4d}$$

with boundary conditions

$$\begin{gathered}\bar{y}=0 \quad u_0 = u_w; \quad v_0 = 0; \quad H_0 = 2H_w\varepsilon^2/U_\infty{}^2 \\ \bar{y}=\infty \quad u_0 = \varepsilon; \quad v_0 = O; \quad H_0 = \varepsilon^2; \quad p_0 = 1/\varepsilon\end{gathered}$$

The first-order approximation (coefficients of ε^1) is continuity:

$$\frac{\partial}{\partial\bar{x}}(\bar{\rho}u_1) + \frac{\partial}{\partial\bar{y}}(\bar{\rho}v_1) = 0 \tag{5a}$$

$\bar{x}$ momentum:

$$\left(u_0\frac{\partial}{\partial\bar{x}} + v_0\frac{\partial}{\partial\bar{y}}\right)u_1 + \left(u_1\frac{\partial}{\partial\bar{x}} + v_1\frac{\partial}{\partial\bar{y}}\right)u_0 = -\frac{1}{\bar{\rho}M_\infty{}^2}\left[\frac{1}{\gamma}\frac{\partial p_0}{\partial\bar{x}} - \frac{4}{3}\frac{\partial}{\partial\bar{x}}\left(\mu_0\frac{\partial u_0}{\partial\bar{x}}\right) + \frac{2}{3}\frac{\partial}{\partial\bar{x}}\left(\mu_0\frac{\partial v_0}{\partial\bar{y}}\right) - \frac{\partial}{\partial\bar{y}}\left(\mu_0\frac{\partial v_0}{\partial\bar{y}}\right) - \frac{\partial}{\partial\bar{y}}\left(\mu_0\frac{\partial u_1}{\partial\bar{y}}\right)\right] \tag{5b}$$

$\bar{y}$ momentum:

$$\left(u_0\frac{\partial}{\partial\bar{x}} + v_0\frac{\partial}{\partial\bar{y}}\right)v_1 + \left(u_1\frac{\partial}{\partial\bar{x}} + v_1\frac{\partial}{\partial\bar{y}}\right)v_0 = \frac{1}{\bar{\rho}M_\infty{}^2}\left[\frac{\partial}{\partial\bar{x}}\left(\mu_0\frac{\partial v_0}{\partial\bar{x}}\right) + \frac{4}{3}\frac{\partial}{\partial\bar{y}}\left(\mu_0\frac{\partial v_1}{\partial\bar{y}}\right) - \frac{2}{3}\frac{\partial}{\partial\bar{y}}\left(\mu_0\frac{\partial u_1}{\partial\bar{x}}\right) + \frac{\partial}{\partial\bar{x}}\left(\mu_0\frac{\partial u_1}{\partial\bar{y}}\right)\right] \tag{5c}$$

energy:

$$\left(u_0\frac{\partial}{\partial\bar{x}} + v_0\frac{\partial}{\partial\bar{y}}\right)H_1 + \left(u_1\frac{\partial}{\partial\bar{x}} + v_1\frac{\partial}{\partial\bar{y}}\right)H_0 = \frac{1}{\bar{\rho}M_\infty{}^2}\left[\frac{\partial}{\partial\bar{y}}\left(\mu_0\frac{\partial H_1}{\partial\bar{y}}\right) + \frac{\partial}{\partial\bar{y}}\left\{\left(\frac{1}{Pr}-1\right)\mu_0\frac{\partial}{\partial\bar{y}}(H_1 - 2u_0u_1)\right\}\right] \tag{5d}$$

with boundary conditions

$$\bar{y}=0 \quad u_1=0; \quad v_1=0; \quad H_1=0$$
$$\bar{y}= \quad u_1=v_1=H_1=0$$

It is seen from system of Eqs. (4) that even in the zeroth approximation, the transfer momentum takes part in determining the flow characteristics in the merged layer. Also system (4) shows that the transverse pressure gradient is of zero order effect. System (5) shows the stream-wise pressure gradient to be of first-order effect (secondary importance in influencing the flow behavior).

Systems (4) and (5) reveal that while the zero-order system of equations are nonlinear, the first-order system of equations are linear (with respect to the first-order variables). To write the governing system of equations in a form more amenable to mathematical analysis, let's introduce the new independent variable η, such that

$$\eta=\frac{1}{\bar{x}}\int_0^{\bar{y}}\bar{\rho}\,d\bar{y} \tag{6}$$

Affecting this change of variables means that the governing equations are to be transfered from the $(\bar{x},\bar{y})$ plane to the $(\bar{x},\eta)$ plane. Also introducing the nondimensional stream function $f(\bar{x},\eta)$ such that

$$f_\eta^{(0)}=u_0; \quad f_\eta^{(1)}=u_1; \quad v_0=(-1/\bar{\rho})[\bar{x}f_{\bar{x}}^{(0)}+f^{(0)}] \tag{7}$$
$$v_1=(-1/\bar{\rho})[\bar{x}f_{\bar{x}}^{(1)}+f^{(1)}] \quad \text{and} \quad f(\bar{x},\eta)=f^{(0)}\varepsilon^{-1}+f^{(1)} \tag{8}$$

where superscripts denote order of approximation. Employing the transformation, we obtain (for compactness, we write only the zero-order equations)

$\bar{x}$ momentum:

$$\left(\frac{\bar{\rho}}{M_\infty^2}\,\mu_0 f_{\eta\eta}^{(0)}\right)_\eta+\bar{x}f^{(0)}f_{\eta\eta}^{(0)}=\bar{x}^2(f_{\eta\eta}^{(0)}f_{\eta\bar{x}}^{(0)}-f_{\bar{x}}^{(0)}f_{\eta\eta}^{(0)}) \tag{9a}$$

η momentum:

$$\bar{x}f_{\bar{x}}^{(0)}f_{\bar{x}\eta}^{(0)}+f^{(0)}f_{\bar{x}\eta}^{(0)}+\frac{1}{\bar{x}}f^{(0)}f_\eta^{(0)}-\bar{x}f_\eta^{(0)}f_{\bar{x}\bar{x}}^{(0)}+f_\eta^{(0)}f_{\bar{x}}^{(0)}=$$

$$\frac{-\bar{\rho}}{\bar{x}M_\infty^2}\left\{\frac{1}{\gamma}\frac{\partial p_0}{\partial\eta}+\frac{2}{3}(\mu_0 f_{\eta\bar{x}}^{(0)})_\eta-(\mu_0 f_{\eta\eta}^{(0)})_{\bar{x}}+(\mu_0 f_{\eta\eta}^{(0)})\frac{1}{\bar{x}}-\frac{4}{3}\left[\bar{\rho}\mu_0\left(f_{\bar{x}\eta\eta}^{(0)}+\frac{1}{\bar{x}}f_{\eta\eta}^{(0)}\right)\right]\right\} \tag{9b}$$

energy:

$$f_\eta^{(0)}H_{\bar{x}}^{(0)}-f_{\bar{x}}^{(0)}H_\eta^{(0)}-\frac{1}{\bar{x}}f^{(0)}H_\eta^{(0)}=\frac{\bar{\rho}}{\bar{x}^2M_\infty^2}\left\{\mu_{0\eta}H_\eta^{(0)}+\mu_0 H_{\eta\eta}^{(0)}+\left(\frac{1}{Pr}-1\right)[\mu_{0\eta}(H_\eta^{(0)}-2f_\eta^{(0)}f_{\eta\eta}^{(0)})+\mu_0(H_{\eta\eta}^{(0)}-2f_\eta^{(0)}f_{\eta\eta\eta}^{(0)}-2f_{\eta\eta}^{(0)2})]\right\} \tag{9c}$$

with boundary conditions

$$\eta=0; \quad f_\eta^{(0)}=u_w; \quad H^{(0)}=2H_w\varepsilon^2/U_\infty^2$$
$$\eta=\infty; \quad f_\eta^{(0)}=\varepsilon; \quad H^{(0)}=\varepsilon^2; \quad f_{\eta\eta}^{(0)}=0$$

where in deriving the preceding equations, the assumptions $(\bar{\rho}_{\bar{x}}/\bar{\rho})\ll 1$ and $(\bar{\rho}_\eta/\bar{\rho})\ll 1$ have been employed. This is in coordination with the physical phenomenum.

The form of Eqs. (9) suggests a test for whether similarity conditions may prevail or not (at least to zero order). Proceeding for the similarity existance test, we assume the following forms:

$$f^{(0)}=\bar{x}^nF(\eta); \quad H^{(0)}=\bar{x}^mg(\eta); \quad \mu_0=\bar{x}^m\alpha(\eta) \tag{10}$$

where n and m are constant quantities.

Substituting into system of Eqs. (9), we see that similarity exists for momentum and energy, whenever one of the following set of conditions is satisfied:

$$Pr=1$$
$$m=n+1 \tag{11}$$
$$p_0=\eta\bar{x}^{(m+n-1)}+\pi(x)$$

or

$$Pr=\text{any constant other than unity}$$
$$n=1; \quad m=2 \tag{12}$$
$$p_0=\eta\bar{x}^{(m+n-1)}+\pi(x)$$

Either of conditions (11) or (12), if satisfied will give complete similarity (similarity in both momentum and energy).

Condition (11) shows that an infinite combinations of values of the constants m and n give similarity. To see, if either of the similar situations stated previously could really exist, we first should bear in mind that the merged region is bounded by $0<\bar{x}<0(1)$, i.e. near the kinetiocregion (lower bound), $\bar{x}$ is mainly a fraction. In this domain (adjacent to the kinetic region) condition (12), if realized, will give increasing wall shear stress, and heat transfer in the downstream direction. The same situation will prevail in the domain adjacent to the strong interaction region (but with different proportions). Such behavior violates the physical trend. Consequently, condition (12) can't truely simulate the physical problem, since the wall shear stress and heat transfer should decrease in the downstream direction. On the other hand, condition (11) may give solutions whose general trend coincides with the characteristics of the flowfield, if and only if, the constants n and m satisfy the inequalities $n<-1$ and $m<0$.

If condition (11) is to exist, Eqs. (9) takes the similar form

$\bar{x}$ momentum:

$$[(\bar{\rho}/M_\infty^2)\alpha F'']'+(n+1)FF''=nF'^2 \tag{13a}$$

η momentum:

$$(3n+1)FF'=-(\bar{\rho}/M_\infty^2)[1/\gamma+\tfrac{2}{3}n(\alpha F')'-\tfrac{4}{3}(n+1)\alpha F''] \tag{13b}$$

energy:

$$(n+1)[gF'-g'F]=(\bar{\rho}/M_\infty^2)[\alpha' g'+\alpha g''] \tag{13c}$$

where in the preceding equations primes denote differentiations with respect to η. In the above derivations, the assumptions of negligible variation of $\bar{\rho}$ with $\bar{x}$ and η was employed.

Equation (13a) although, similar in form to the conventional boundary layer equation, it gives inconsistent description of the flowfield. In order to satisfy condition (11), the inequalities, $(n+1)<0$ and $n<-1$, must be enforced. Employing such conditions to Eq. (13a) reveals that the inertia force and the viscous force are in the same direction, a situation, which violates the physical behavior. Moreover, the stream-wise pressure gradient term is shown to adverse, which in itself contradicts condition (11). This gives enough evidence that the similar Eqs. (13) fail to describe adequately the flow parameters variations in the transverse direction of the merged layer region.

Conclusion

The similar solution approach has shown that although it yields proper variations of flow parameters in the stream-wise direction, it fails to predicts such variations in the transverse direction.

The conclusion that can be drawn from this analysis is that determination of the flow characteristics in the merged layer region should be accomplished by solving the complete zero order Eqs. (9). More accurate results can be obtained by adding the first order solutions of Eqs. (5) and (6). As well realized, such solutions can only be achieved by numerical means.

References

[1] Garvine, R. W., "Hypersonic Viscous Flow Near a Sharp Leading Edge," *AIAA Journal*, Vol. 2, No. 9, Sept. 1964, pp. 1660–1661.

[2] Waldron, H. F., "Viscous Hypersonic Flow Over Pointed Cones at Low Reynolds Numbers," *AIAA Journal*, Vol. 5, No. 2, Feb. 1967, pp. 208–218.

[3] Raat, J. and Pasiuk, L., "Rarefaction Effects in Hypersonic Boundary Layers," *AIAA Journal*, Vol. 4, No. 11, Nov. 1966, pp. 2052–2054.

[4] Hakure, O., "Leading Edge Effects in Rarefied Hypersonic Flow," *Rarefied Gas Dynamics*, edited by J. A. Laurmann, Vol. II, 1963, pp. 181–193.

[5] Shoronstein, M. L. and Probstein, R. F., "Hypersonic Leading Edge Problem," *AIAA Journal*, Vol. 6, No. 10, Oct. 1968, pp. 1898–1906.

An Advanced Stochastic Model for Threshold Crossing Studies of Rotor Blade Vibrations

GOPAL H. GAONKAR*
Southern Illinois University, Edwardsville, Ill.
AND
KURT H. HOHENEMSER †
Washington University, St. Louis, Mo.

A STOCHASTIC model to analyze turbulence excited rotor blade vibrations, previously described by the authors, has been generalized and amplified to include nonuniformity of the atmospheric turbulence velocity across the rotor disk in longitudinal direction.

The authors[1] have previously solved the problem of threshold crossing expectations of rotor blade flapping response to atmospheric turbulence. The theory pertained to high rotor advance ratios and low-rotor lift, where a linear description is adequate and where turbulence excited blade vibrations are severe. In the earlier stochastic model it has been assumed that the vertical turbulence velocity at a given point in time is uniform over the rotor disc. This assumption limited the theory to turbulence scale lengths which are large as compared to the rotor radius. In the following a less restrictive stochastic model is described where correlations between vertical turbulence velocities across the rotor disk in the longitudinal direction are considered.

As before, the widely used von Kármán vertical turbulence spectrum is approximated by one with an exponential autocorrelation function and zero mean

$$R_\lambda(\tau)/{\sigma_\lambda}^2 = \exp -|r|\,2/L \tag{1}$$

The associated two-sided spatial power spectral density is

$$\{S_\lambda(\omega_r)/{\sigma_\lambda}^2\}\,d\omega_r = \{2L/\pi[4+(\omega_r L)^2]\}\,d\omega_r \tag{2}$$

$\lambda = w/\Omega R$ is the dimensionless vertical turbulence velocity, Ω is the angular rotor speed, R the rotor radius, L is the longitudinal turbulence scale, $L/2$ the vertical turbulence scale. The integral over Eq. (2) from $-\infty$ to $+\infty$ is one. If r is the longitudinal displacement of the rotor center and if the flight velocity V is uniform, we have $r = Vt/\Omega$, where t is the dimensionless time with $1/\Omega$ as time unit. Defining the timewise dimensionless circular frequency ω associated with the spatial circular frequency ω_r by $\omega\Omega = \omega_r V$, one obtains from Eq. (2) the two-sided timewise power spectral density for the nondimensional vertical turbulence velocity λ

$$\{S_\lambda(\omega)/{\sigma_\lambda}^2\}\,d\omega = \{a/\pi(a^2+\omega^2)\}\,d\omega \tag{3}$$

where

$$a = 2V/\Omega L = 2\mu/(L/R) \tag{4}$$

Received January 14, 1972. Sponsored by the Ames Directorate, AAMRDL under Contract NAS2-4151.

Index categories: VTOL Structural Design (Including Loads); VTOL Vibration; Structural Dynamic Analysis.

* Visiting Research Professor.

† Professor of Aerospace Engineering. Associate Fellow AIAA.

$\mu = V/\Omega R$ is the rotor advance ratio. The spectrum Eq. (3) can be obtained by passing white noise through the first order filter

$$\dot\lambda + a\lambda = \sigma_\lambda(2a)^{1/2}n, \quad \text{with} \quad R_n(\tau) = \delta(\tau) \tag{5}$$

The integral over Eq. (3) from $-\infty$ to $+\infty$ is again one. Assuming that the dynamics of the rotor is given in state variable form by

$$\dot X(t) = A(t)\,X(t) + B(t)\,\lambda(t) \tag{6}$$

where $X(t)$ is the state vector with components $X_1, X_2, \ldots$ and with initial state $X(0)$, where $A(t)$ is the periodic state matrix, where $B(t)$ is the periodic coupling matrix relating the input vector $\lambda(t)$ assumed to have zero mean to the rate of state vector, one can express the response covariance matrix by

$$R_{xx}(t_1,t_2) = \int_{-\infty}^{\infty} H^*(\omega,t_1)S_\lambda(\omega)H^T(\omega,t_2)\,d\omega \tag{7}$$

$H(\omega,t)$ is the response vector to the input $\lambda(t) = u(t)\exp i\omega t$, $u(t)$ being the unit step function. Equations (6) and (7) are matrix generalizations to the expressions given earlier.[1] For the blade flapping problem $X_1 = \beta, X_2 = \dot\beta, \dot X_1 = \dot\beta, \dot X_2 = \ddot\beta$ etc. Once the response covariance matrix is known, and assuming that the input $\lambda(t)$ is Gaussian, it is easy to compute the threshold crossing expectations for any response quantity.[1,2] If $X_i = \dot X_k$, then the expected number of positive crossings of the level ζ per unit time is†

$$\begin{aligned} E_k[N_+(\zeta,t)] = {} & (1/2\pi)(1-{r_{ik}}^2)^{1/2}(\sigma_i/\sigma_k)\times \\ & \exp[-(\zeta/\sigma_k)^2/2(1-{r_{ik}}^2)] + \\ & [1/2(2\pi)^{1/2}](\sigma_i/\sigma_k)(\zeta r_{ik}/\sigma_k)\{\exp[-(\zeta^2/2{\sigma_k}^2)]\}\times \\ & (1+\operatorname{erf}\{\zeta r_{ik}/\sigma_k[2(1-{r_{ik}}^2)^{1/2}]\}) \end{aligned} \tag{8}$$

If the filter Eq. (5) is included in the dynamic matrix Eq. (6) one has the case of white noise input, for which the response variance $R_{xx}(t,t) = P(t)$ can be determined from[3-5]

$$\dot P(t) = A(t)P(t) + P(t)A^T(t) + B(t)B^T(t) \tag{9}$$

with zero initial state. The response covariance matrix is then obtained from

$$R_{xx}(t_1,t_2) = \begin{cases} \Phi(t_1,t_2)P(t_2), & t_1 \geqslant t_2 \\ P(t_1)\Phi^T(t_2,t_1), & t_1 \leqq t_2 \end{cases} \tag{10}$$

where $\dot\Phi(t,\tau)$ is the state transition matrix defined by $\dot\Phi(t,\tau) = A(t)\Phi(t,\tau)$, $\Phi(\tau,\tau) = I$. Under certain conditions the evaluation of Eqs. (9) and (10) requires less computational effort than that of Eq. (7).

So far we have merely generalized the previous stochastic model[1] to arbitrary many degrees of freedom. Now let us assume that the blade, instead of being subjected at each point in time to the vertical turbulence velocity λ at the rotor center, is subjected to the turbulence velocity at the 0.7 radius station, whereby this velocity is assumed to be uniform in the lateral direction, an assumption often made in aircraft turbulence response analysis. We now determine the response of the rotor blade as it passes through a space wave,

$$\lambda(r) = u(r)\exp i\omega_r r \tag{11}$$

With the previous assumptions $r = Vt/\Omega$ and $\omega\Omega = \omega_r V$ this is

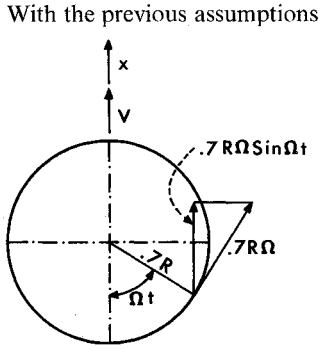

Fig. 1 Forward component of blade velocity at 0.7*R*.

† Equation (30) in Ref. 1, which corresponds to Eq. (8) herein has two printing errors: $\frac{1}{2}\pi$ should be $\frac{1}{2}\pi$, $\frac{1}{2}(2\pi)^{1/2}$ should be $\frac{1}{2}(2\pi)^{1/2}$.